Journal of Alzheimer's Disease Reports 7 (2023) 1313–1322
DOI 10.3233/ADR-230076
IOS Press

Research Report

Skipping of *FCER1G* Exon 2 Is Common in Human Brain But Not Associated with the Alzheimer's Disease Genetic Risk Factor rs2070902

Alyssa C. Feldner, Andrew K. Turner, James F. Simpson and Steven Estus*
Department of Physiology and Sanders-Brown Center on Aging, University of Kentucky, Lexington, KY, USA

Received 20 July 2023
Accepted 30 October 2023
Published 30 November 2023

Abstract.
Background: Understanding the mechanisms whereby genetic variants influence the risk of Alzheimer's disease (AD) may provide insights into treatments that could reduce AD risk.
Objective: Here, we sought to test the hypothesis that a single nucleotide polymorphism (SNP) associated with AD risk, rs2070902, influences splicing of *FCER1G* exon 2.
Methods: AD and non-AD brain samples were analyzed for *FCER1G* expression by genotyping, immunohistochemistry, immunofluorescence, and qPCR.
Results: The protein encoded by *FCER1G,* FcRγ, is robustly expressed in microglia in both AD and non-AD brain. The *FCER1G* isoform lacking exon 2 (*D2-FCER1G*) was readily detectable. Moreover, the proportion of *FCER1G* expressed as this isoform was increased in brains with high AD neuropathology. However, the proportion of *FCER1G* expressed as the *D2-FCER1G* isoform was not associated with rs2070902 genotype.
Conclusions: In summary, the proportion of *FCER1G* expressed as the *D2-FCER1G* isoform is increased with AD neuropathology but is not associated with rs2070902.

Keywords: Alzheimer's disease, genetics, microglia, polymorphism, RNA splicing

INTRODUCTION

Genome-wide association studies have identified a set of polymorphisms that are associated with AD risk [1–6] by revealing single nucleotide polymorphisms (SNPs) with a statistically significant difference in allele frequency between AD and non-AD populations. Hence, these SNPs modulate AD risk but are not sufficient to cause AD. Among these SNPs is rs2070902 which is located within the gene *FCER1G* [2]. This SNP has a minor allele frequency of 25%, 37%, and 43% in Caucasians, Africans, and Asians, respectively. Within the Caucasian subjects involved with this study, the rs2070902 major allele homozygous CC individuals were 56% of the population, heterozygous CT individuals 36%, and homozygous

*Correspondence to: Steven Estus, Department of Physiology and Sanders-Brown Center on Aging, University of Kentucky, 789 S Limestone St., Lexington, KY 405361, USA. E-mail: steve.estus@uky.edu.

ISSN 2542-4823 © 2023 – The authors. Published by IOS Press. This is an Open Access article distributed under the terms of the Creative Commons Attribution-NonCommercial License (CC BY-NC 4.0).

TT individuals 6%. Whether rs2070902 acts through *FCER1G* or is a proxy for other SNPs in the region that act on neighboring genes, including *ADAMTS4*, is unclear [2].

The protein encoded by *FCER1G*, Fc receptor gamma chain (FcRγ) [7], is a signaling adaptor that pairs with multiple receptors, including FcεRI, FcγRI, FcγRIIIa, FcαRI, GPVI, OSCAR, PIR-A, Dectin-2, γδTCR, and IL-3R [8]. Many of these receptors are expressed in microglia, including FcεRI, FcγRI, FcγRIIIa, FcαRI, and OSCAR [9]. Ligand binding to the receptor complex results in phosphorylation of the FcRγ immunoreceptor tyrosine-based activation motif (ITAM), which leads to activation of SYK, CARD9 and NF-kappa-B in a process that appears to parallel that of activated TREM2 [8, 9], another gene linked to AD risk by genetics [10]. Whether *FCER1G* expression is altered in AD has not been reported. However, *FCER1G* has been reported to be upregulated in two murine models of AD as part of a larger network of microglia gene expression changes in these models [11, 12]. Indeed, *FCER1G* expression is increased approximately 50% in disease-associated microglia, relative to homeostatic microglia [13]. In summary, FcRγ signals through an ITAM that, at least in the case of TREM2, affects microglial activation and influences AD risk. However, the effects of genetics or AD status on *FCER1G* expression in the human brain has not yet been reported.

Since rs2070902 is located 16 base pairs (bp) upstream of exon 2 in *FCER1G*, Schwartzentruber et al. hypothesized that rs2070902 may affect exon 2 splicing [2]. To test this hypothesis, we quantified the expression of *FCER1G* with exon 2 present (P2-FCER1G) and with exon 2 deleted (*D2-FCER1G*) in a series of human AD and non-AD brains. We report FcRγ is robustly expressed in microglia and that *D2-FCER1G* is a common *FCER1G* isoform. Moreover, expression of *D2-FCER1G* is increased in brains of individuals with high AD neuropathology. However, we did not detect an association between rs2070902 and *FCER1G* exon 2 splicing.

MATERIALS AND METHODS

Human brain DNA and cDNA

Genomic DNA and RNA for this study were obtained from autopsied anterior cingulate brain samples and the RNA converted to cDNA as previously described [14–17]. The anterior cingulate cortex was used because the area is moderately affected in AD but does not have extensive neuronal death that could skew cell type-specific RNA proportions [18]. The National Institute on Aging-Reagan Institute (NIARI) criteria for neuropathological diagnosis of AD based on amyloid and tau deposition were used as a measure of AD neuropathology, where samples from brains with a score of "intermediate likelihood" or below were defined as low AD neuropathology ($n = 28$), and samples from brains with a score of "high likelihood" were defined as high AD neuropathology ($n = 26$) (reviewed in [19]). The age at death of the high pathology individuals was 82.0 ± 6.4 (mean $\pm$ SD) and that of the low pathology individuals was 82.6 ± 8.7. The postmortem intervals for the high and low pathology samples were similar, 3.5 ± 0.6 and 2.7 ± 0.8 h, respectively.

The study was conducted according to the guidelines of the Declaration of Helsinki and approved by the Institutional Review Board at the University of Kentucky (2018–3028).

Immunohistochemistry

Formalin-fixed paraffin embedded coronal sections were deparaffinized through consecutive washes in SafeClear solution and decreasing concentrations of ethanol. Following a PBS wash, sections were subjected to antigen retrieval in citrate buffer (pH 6.0) for 30 min at 95°C and then washed in PBS. Endogenous peroxidase was quenched by washing slides in 3% hydrogen peroxide in methanol for 30 min. Sections were blocked in PBS with 10% horse serum and 0.1% Tween-20 for 2 h at room temperature. Slides were then incubated with an antibody against FcRγ (ab: 06-727, Millipore) at a 1:1000 dilution in the blocking solution overnight at 4°C in a humidified chamber. Slides were washed in PBS containing 0.1% Tween-20 and incubated with a biotinylated secondary antibody (BA-1400-2.1, Vector Laboratories) at a 1:50 dilution in blocking buffer for 30 min at room temperature. Then sections were washed in PBS, incubated in biotin amplification solution (ABC Elite kit, Vector Laboratories) for 30 min, and staining developed by using DAB peroxidase substrate kit (Vector Laboratories). To label for amyloid-beta, slides were washed in 3% hydrogen peroxide in methanol for 30 min, washed in PBS, incubated with blocking buffer for 1 h, washed in PBS, and incubated with an amyloid-beta antibody (6E10, Covance) at a 1:500 dilution overnight at 4°C. The slides were then incubated

for 30 minutes at room temperature with a biotinylated secondary antibody, washed in PBS, incubated in biotin amplification solution, washed in PBS, and staining developed by using an SG peroxidase substrate kit (Vector Laboratories). Sections were then dehydrated through increasing concentrations of ethanol and SafeClear solution. The slides were then mounted, cover-slipped and representative images obtained on an Olympus BX51 microscope with a 40× objective.

Immunofluorescence

Formalin-fixed paraffin embedded coronal sections were deparaffinized and subjected to antigen retrieval as described above. Sections were blocked in PBS with 10% horse serum and 0.1% Tween-20 for 2 h at room temperature. Slides were then incubated with an antibody against FcRγ (ab: 06-727, Millipore) at a 1:1000 dilution and an IBA1 antibody (ab5076, Abcam) at a 1:100 dilution in the blocking solution overnight at 4°C in a humidified chamber. Slides were washed in PBS containing 0.1% Tween-20 and incubated with an Alexa Fluor 488 nm donkey anti-goat secondary antibody (RRID:AB_2534102, ThermoFisher) at a 1:1000 dilution and an Alexa Fluor 594 nm donkey anti-rabbit (RRID:AB_2340621, Jackson ImmunoResearch) at a 1:500 dilution in blocking buffer for 1 h at room temperature. Sections were then washed in PBS and mounted with Prolong Glass with NucBlue (ThermoFisher). Fluorescence was then visualized by confocal microscopy (Nikon A1R HD) and representative images obtained with a 40× objective.

PCR

Genomic DNA samples were genotyped for rs2070902 using TaqMan Genotyping (Thermo) as directed by the manufacturer: initial genomic denaturation at 98°C for 30 s, and PCR cycling at 98°C, 10 s; 60°C, 1 min; 40 cycles. To identify *FCER1G* splice variants in human brain, cDNA samples corresponding to 30 ng of RNA from eight individuals (4 AD; 4 non-AD) were subjected to polymerase chain reaction (PCR) with primers corresponding to sequences within exon 1 and exon 5, GGCCGATCTCCAGCCCAAG and ACAGGGAGGAGGAACCACTG, respectively. After 28 cycles with Platinum Taq DNA Polymerase (Thermo), PCR products were separated by electrophoresis on a 10% polyacrylamide gel and visualized with SYBR Gold staining. The PCR products were excised from the gel, reamplified, and sequenced to confirm their identity (ACGT, Inc).

qPCR

To quantify *FCER1G* with and without exon 2, we used qPCR assays targeting each isoform by using a PerfeCTa SYBR Green master mix and PCR products as standards, an approach previously described [14–17]. *FCER1G* with exon 2 present (*P2-FCER1G*) was quantified using primers corresponding to sequences within exons 1 and 2, TGATTCCAGCAGTGGTCTTGC and GTAGAGGAGGGTGAGGACAAT, respectively. *FCER1G* lacking exon 2 (*D2-FCER1G*) was quantified using primers corresponding to exon 1 and the exon 1–3 junction, CTCCAGCCCAAGATGATT and TCGCACTTGGATCTGCTT, respectively. Total *FCER1G* was quantified as the summation of *P2-FCER1G* and *D2-FCER1G*. *AIF-1* and *ITGAM* expression were quantified as described [20]. For each assay, copy numbers present in cDNA samples were determined relative to standard curves executed in parallel [15–17]. The standard curves were generated with a quantified PCR product that was serially diluted.

Statistics

Since *FCER1G* expression was restricted to microglia and the proportion of microglial cells can vary among samples, *FCER1G* expression was compared to the geometric mean of the microglial genes *AIF-1* and *ITGAM* by using linear regression of the log-normalized copy number values. To determine the effects of AD neuropathology and rs2070902 status on *FCER1G* expression, we then analyzed the ratio of *FCER1G* : geometric mean of *AIF-1* and *ITGAM* by using a general linear model (SPSS versus 28). Similarly, the expression of *D2-FCER1G* was compared to *P2-FCER1G* by using linear regression of the log-normalized copy number values. The effects of AD neuropathology and rs2070902 genotype on the ratio of *D2-FCER1G: P2-FCER1G* was then analyzed by using a general linear model. As noted above in the description of these brain samples, AD neuropathology was modeled as high versus low pathology. Rs2070902 was modeled as major allele CC homozygotes ($n = 28$) versus minor allele T carriers (CT and TT combined, $n = 26$).

RESULTS

The overall experimental design of this study can be outlined in three steps. First, we focused on FcRγ protein expression in the human brain with and without AD pathology. Second, we identified the *FCER1G* isoforms that are expressed in these brains. Third, we compared expression of these *FCER1G* isoforms in brains as a function of AD neuropathology and AD genetics (rs2070902).

Prior immunostaining studies reported that FcRγ is expressed in cells with microglial morphology [21, 22]. Consistent with this finding, single cell RNAseq studies indicate that *FCER1G* expression is restricted to microglia [23]. To confirm and extend these findings, we performed a double-label study wherein human brain sections were immunolabeled for both FcRγ and for IBA1, a well-known microglial protein (Fig. 1). We found that antibodies against FcRγ (red) and IBA1 (green) labeled the same population of cells (yellow). Microglial morphology included both highly ramified and amoeboid microglia. In summary, FcRγ was robustly expressed in microglia in both AD and non-AD brain tissue (Fig. 1).

We next examined microglial FcRγ expression in the presence and absence of senile plaques. For this effort, brain sections were doubled-labeled for FcRγ and the principal proteinaceous component of senile plaques, amyloid-beta. Microglia express FcRγ robustly regardless of their proximity to amyloid plaques, as shown in a non-AD brain (Fig. 2A) and in an AD brain (Fig. 2B).

To begin to evaluate *FCER1G* expression and genetics, we first identified the primary *FCER1G* isoforms present in AD and non-AD brains. The prototypic *FCER1G* isoform consists of five exons that encode a protein consisting of 86 amino acids [24, 25] (Fig. 3A). Schwartzentruber et al. suggested that rs2070902 may be associated with the splicing efficiency of exon 2 because rs2070902 is within the first intron, 16 bp before exon 2 [2]. To qualitatively determine the primary *FCER1G* splicing variants in human brain as a function of AD status and rs2070902, we performed PCR with primers corresponding to sequence within exon 1 and exon 5. For this study, we used cDNA prepared from RNA isolated from AD and non-AD human brain samples that were homozygous for the rs2070902 major allele (CC), heterozygous (CT) or homozygous for the minor allele (TT) (Fig. 3B). With this approach, the predominant PCR product for all the samples was found to correspond to the canonical full-length, five-exon *FCER1G,* which manifests as a 440 bp PCR product (Fig. 3B). The second most abundant isoform corresponds to *D2-FCER1G* and migrates at 348bp (Fig. 3B). The identities of these PCR products were confirmed by direct sequencing. Note that direct sequencing also established that the PCR product marked by an asterisk was derived from *HSPA1B* and hence represents a non-specific product. Overall, we interpreted this qualitative result as indicating that exon 2 skipping was moderately common in human brain and that exons 3 and 4 were constitutively present.

Exon 2 encodes a large proportion of FcRγ, including the signal peptide, short FcRγ extracellular domain, transmembrane domain, and part of the cytosolic domain (Fig. 3C). Hence, loss of exon 2 deletes these structures from FcRγ. Moreover, loss of the 92-bp exon 2 results in a codon reading frameshift and a premature termination codon. Hence, the ITAM encoded by exons 4 and 5 is also not present in D2-FCER1G. Instead, *D2-FCER1G* encodes a short peptide consisting largely of the signal peptide and likely represents a complete loss of FcRγ protein function (Fig. 3C).

To quantify the expression of *FCER1G* with exon 2 present (*P2-FCER1G*) and without exon 2 (*D2-FCER1G*), qPCR assays were developed that were specific to each isoform. Total *FCER1G* was defined as the sum of *P2-FCER1G* and *D2-FCER1G*. The cDNA samples were grouped as either low or high AD neuropathology and as either homozygous for the major C allele of rs2070902, or as rs2070902 minor allele carriers (CT and TT). Since FCER1G expression is robust in microglia (Figs. 1 and 2), we compared *FCER1G* expression with the geometric mean of the microglial genes *AIF-1* and *ITGAM*. Total *FCER1G* expression strongly correlated with microglial gene expression ($p < 0.0001$, $r^2 = 0.740$, Fig. 4A). Comparison of the ratio of total *FCER1G* to microglial gene expression found that total *FCER1G* was modestly increased with AD neuropathology ($p = 0.04$, $F_{1,51} = 4.27$) but not with the AD-associated SNP ($p > 0.05$, Fig. 4B). Expression of *FCER1G* with exon 2 present strongly correlated with expression of *FCER1G* with exon 2 skipped ($p < 0.0001$, $r^2 = 0.563$, Fig. 4C). Comparison of the ratio of *D2-FCER1G* to *P2- FCER1G* found an increase in *D2-FCER1G* with AD neuropathology ($p = 0.02$, $F_{1,51} = 5.80$) but not with the AD-associated SNP ($p > 0.05$, Fig. 4D). Quantitatively, the *D2-FCER1G : P2-FCER1G* ratio

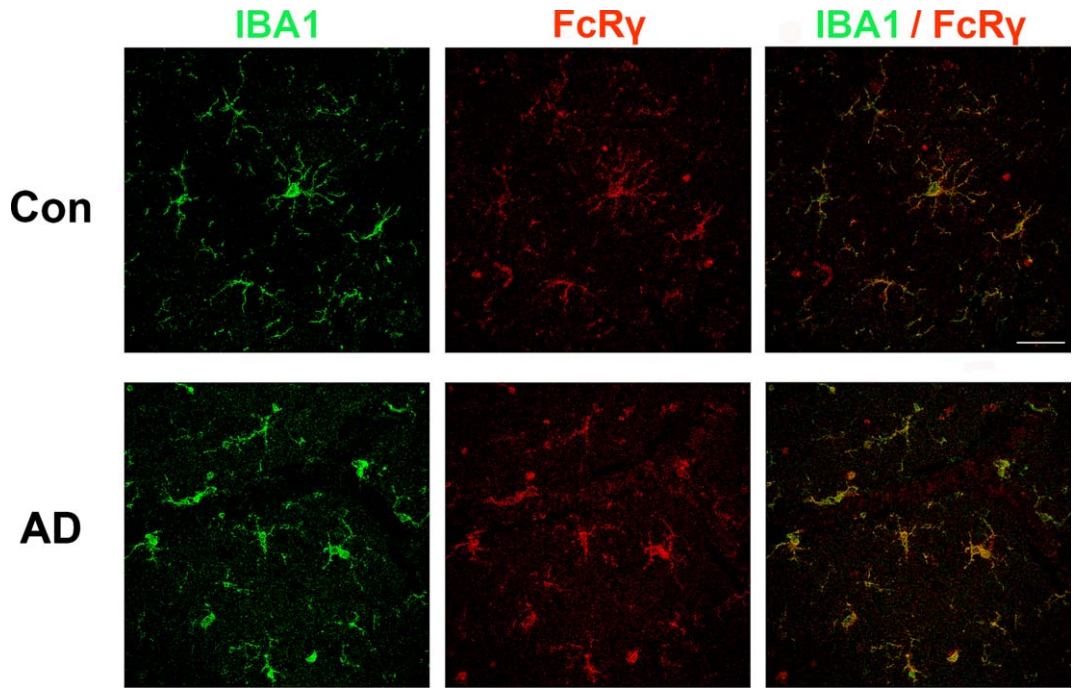

Fig. 1. FcRγ and IBA1 co-expression in human brain. Brains sections from individuals with or without AD were immunolabeled for IBA1 (green) and FCER1G (red). The merged image at the right shows that cells labeled by FcRγ are also labeled by IBA1, consistent with the concept that FcRγ is primarily expressed by microglia in the brain. Scale bar = 50 μm.

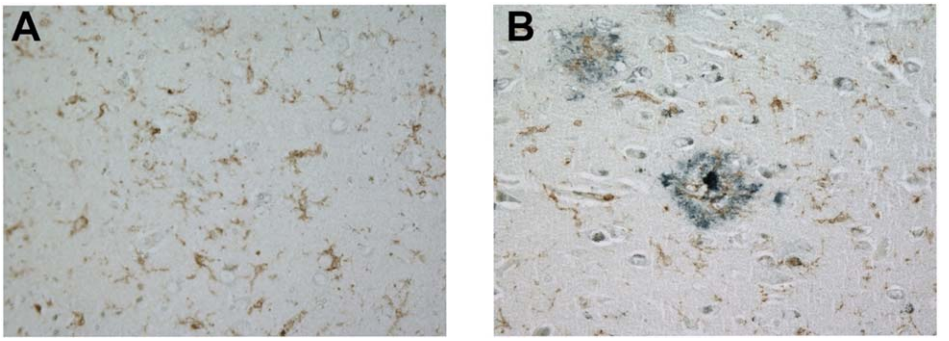

Fig. 2. FcRγ is expressed robustly in a non-AD brain in the absence of amyloid plaques (A) and in an AD brain in the presence of amyloid plaques (B). These representative images were obtained with a 40× objective. Brown label represents FcRγ staining while blue-black label represents amyloid-beta staining.

changed from 0.144 ± 0.081 (mean $\pm$ SD, $n = 28$) to 0.208 ± 0.111 (mean $\pm$ SD, $n = 26$) for low and high AD neuropathology samples, respectively.

DISCUSSION

The primary findings of this study are three-fold. First, FcRγ is robustly expressed in human microglia *in vivo*. Second, *FCER1G* lacking exon 2 represents approximately 15% of total *FCER1G* expression and the proportion of *FCER1G* expressed as this isoform is significantly increased in brains with high AD neuropathology. Since *D2-FCER1G* encodes a signal peptide but lacks the FcRγ ITAM, we predict that *D2-FCER1G* represents a loss of function relative to *P2-FCER1G*. Lastly, rs2070902 is not associated with *FCER1G* splicing. Hence, this SNP is associated with AD by genetics but does not appear to impact total *FCER1G* expression or *FCER1G* splicing. In summary, *D2-FCER1G* is commonly present

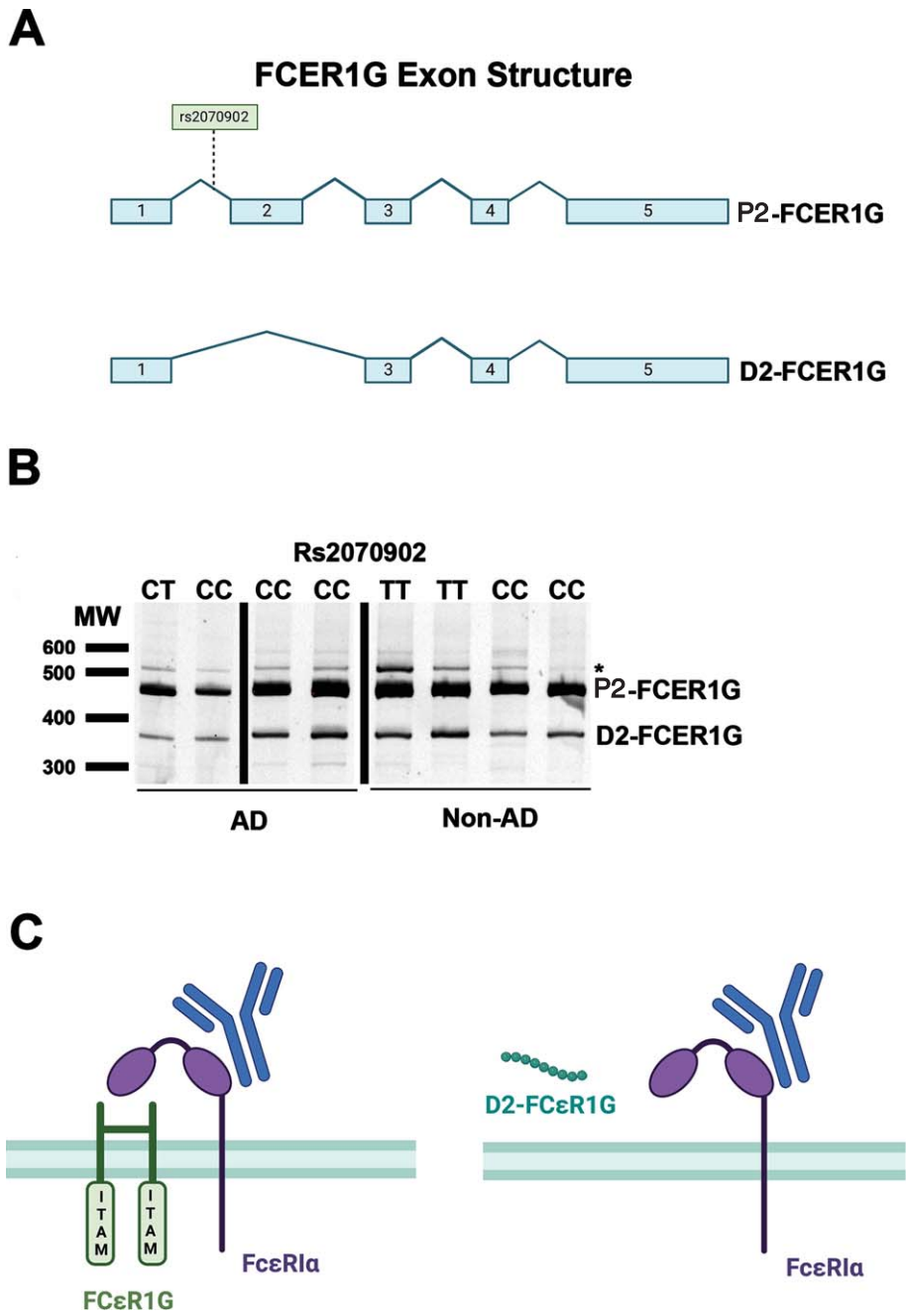

Fig. 3. *FCER1G* isoforms present in human brain. Canonical *FCER1G* consists of five exons (A). PCR amplification from exon 1 to exon 5 in AD and non-AD brain samples with different rs2070902 genotypes (CC, CT, or TT) generated qualitatively similar results in that (i) the primary *FCER1G* isoform consists of prototypic *FCER1G* that contains exons 1, 2, 3, 4, and 5, and (ii) *D2-FCER1G*, which lacks exon 2, was the primary variant *FCER1G* isoform and was present regardless of AD neuropathology or rs2070902 genotype status (B). Note that these PCR products were directly sequenced to confirm the identities of *P2-FCER1G* and *D2-FCER1G*. Further, the PCR product labeled * was found to be derived from *HSPA1B* and hence represents a non-specific PCR product (B). Prototypic FcRγ exists as a disulfide linked dimer that uses its ITAM domains to mediate signaling from antibody-stimulated FcεRIα (C). Although only FcεRIα is depicted, FcRγ also mediates signaling from other Fc receptors such as FcγRI, FcγRIIIa, and FcαRI as well as immune receptors such as GPVI, OSCAR, PIR-A, Dectin-2, γδTCR, and IL-3R [8]. Loss of *FCER1G* exon 2 results in a premature stop codon such that *D2-FCER1G* encodes only a nine amino acid peptide fragment (C). This fragment consists of the signal peptide sequence and does not include the ITAM domain (C). Hence, the peptide encoded by *D2-FCER1G* appears to represent a complete loss of functional FcRγ.

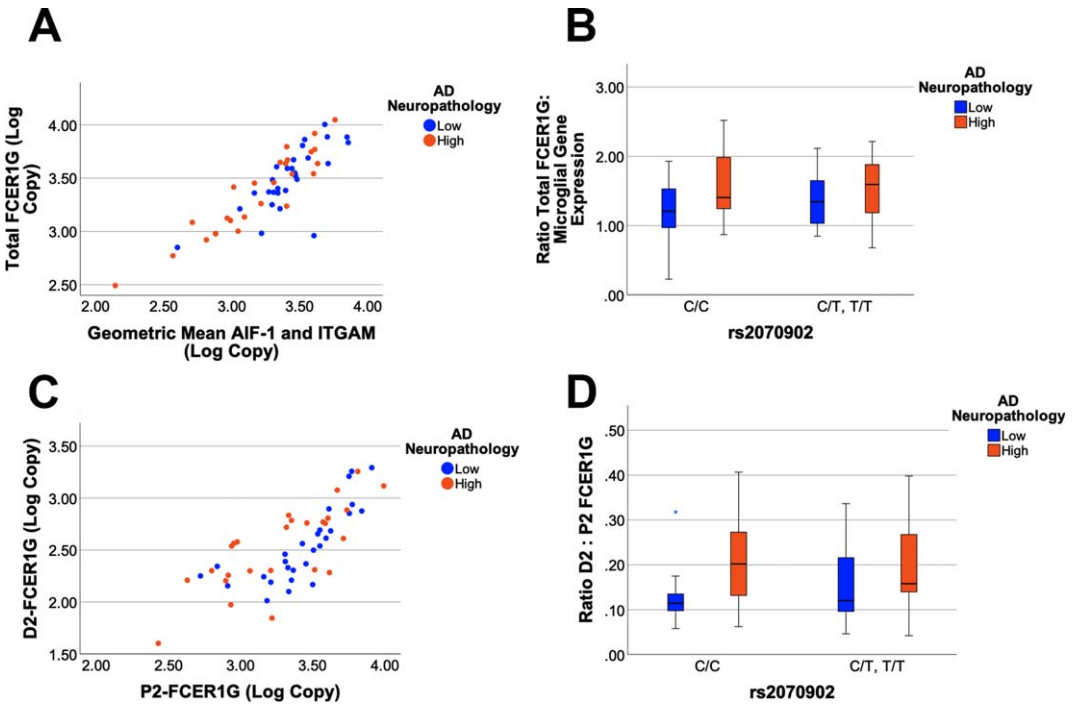

Fig. 4. *FCER1G isoform* expression as a function of AD neuropathology and genetics. Total *FCER1G* expression correlates strongly with the expression of microglial genes ($p < 0.0001$, $r^2 = 0.740$), which are modeled as the geometric mean of mean of *AIF-1* and *ITGAM* expression (A). A General Linear Model analysis found that the ratio of total *FCER1G*: microglial gene expression is increased with AD neuropathology ($p = 0.04$) but not associated with rs2070902 ($p > 0.05$) (B). The expression of *D2-FCER1G* correlated well with *P2-FCER1G* ($p < 0.0001$, $r^2 = 0.563$) (C). The ratio of *D2- FCER1G : P2-FCER1G* expression was increased in samples with high AD neuropathology ($p = 0.02$) but was not associated with rs2070902 ($p > 0.05$) (D). In the box plots, the median and middle interquartile range are represented by the horizontal bar and accompanying box, respectively. The whiskers demarcate 1.5 times the interquartile range while an asterisk (D) denotes outliers beyond this range.

in the human brain and increased in AD but is not by affected by AD genetics.

AD genetic risk factors have been an area of intense scrutiny because they may reveal insights into the mechanisms underlying AD risk. Schwartzentruber et al. identified rs2070902 as associated with AD risk and hypothesized that this SNP may affect *FCER1G* splicing [2]. Our findings did not support this hypothesis because we did not detect an association between the SNP and *D2-FCER1G* expression. We also did not detect an association between total *FCER1G* expression and rs2070902. Thus, *FCER1G* does not appear to mediate the association between rs2070902 and AD risk. Other genes in the vicinity that may mediate this risk should be scrutinized instead, noting that rs2070902 appears associated with expression of *ADAMTS4*, *NDUFS2* and *B4GALT3* in at least a few tissues [26]. Among these candidates, ADAMTS4 has been found to generate N-terminally truncated forms of amyloid-beta peptide, and therefore may be the best target for the actions of rs2070902 relevant to AD [27].

Positive findings from this study included that FcRγ was primarily expressed in microglia in both AD and non-AD brains. Moreover, *D2-FCER1G* was the primary *FCER1G* variant isoform in the brain. Additionally, *D2-FCER1G* was significantly increased in brains with high AD neuropathology. While statistically significant ($p = 0.02$), the extent of this increase was somewhat modest, i.e., the *D2-FCER1G : P2-FCER1G* ratio changed from 0.144 ± 0.081 (mean $\pm$ SD, $n = 28$) to 0.208 ± 0.111 (mean $\pm$ SD, $n = 26$) for low and high AD neuropathology samples, respectively. Since *D2-FCER1G* encodes a peptide that lacks an ITAM and is hence incapable of mediating normal FcRγ signaling, we interpret this result overall as suggesting a modest reduction in *FCER1G* transcripts encoding functional FcRγ in brains with high AD pathology. Whether this change in *FCER1G* splicing is sufficient

to impact microglial function will require further work. For example, a future target of experimentation could be comparison of motility or phagocytosis in cells expressing *FCER1G* normally versus cells hemizygous for *FCER1G* exon 2 deletion. Ultimately, a mouse model that expresses the *D2-FCER1G* isoform may be necessary to definitively show how, if at all, *FCER1G* splicing affects microglial function and AD-related pathology *in vivo*.

Since the loss of exon 2 results in a codon reading frameshift and a premature translation termination codon, the possibility exists that *D2-FCER1G* may undergo nonsense-mediated RNA decay (NMD). Indeed, NMD often occurs when a ribosome encounters a termination codon upstream of an exon junction complex [28]. However, *D2-FCER1G* may not be subject to NMD because mRNA transcripts with translation start sites near premature termination codons commonly escape NMD [29–31]. This occurs because binding of UPF1 to the translation complex is necessary for NMD, and this binding is blocked by the interaction of the poly(A)-binding protein 1 with the eukaryotic translation initiation factors eIF4G and eIF3 [29–31] when the mRNA begins translation. In summary, if *D2-FCER1G is* expressed as protein, the protein would consist of a nine- amino acid peptide. Whether *D2-FCER1G* undergoes NMD is unlikely because of the proximity of the premature termination codon to the translation start site.

FCER1G is a member of a larger gene family that contains ITAMs to mediate signaling. A common model used to study the role of activating FcγRs *in vivo* are mice deficient for this Fcγ chain, who lack expression of functional activating FcγRs. Activating FcγR deficient mice show decreased antibody mediated phagocytosis, abnormal platelet activation and an attenuated immune response to immune complexes [32]. However, some of these effects may be mediated by other immune receptors, such as C-type lectins, which also depend on Fcγ chain signaling [33]. In contrast to activating Fcγ receptors, the expression and therefore function of the inhibitory Fcγ receptor (FcγRIIb) is maintained. Human FcγRIIa carries an intrinsic ITAM in its cytoplasmic domain. Ligation of IgG-immune complexes by activating FcγRs results in the crosslinking of the receptor and the phosphorylation of ITAMs in the cytoplasmic chain. This forms a binding site for the Spleen tyrosine kinase (Syk), which then activates downstream signaling cascades such as the PI3K pathway. Cellular calcium levels are increased, and the cell becomes activated which can result in increased proliferation, cytokine/chemokine release, phagocytosis, and antigen presentation [34]. The inhibitory FcγRIIb signals through an intrinsic cytoplasmic immunotyrosine inhibitory motif (ITIM), cross-linking with an activating receptor results in ITIM phosphorylation leading to the inhibition of cellular activation [34]. The process of FcγR mediated activation or inhibition of an effector cell is outlined in Fig. 1.

The primary limitation of this study may be the number of available brain samples. However, studies involving larger numbers of samples such as those described in Genotype-Tissue Expression (GTEx) have also generally not found an association between rs2070902 and either *FCER1G* splicing or total *FCER1G* expression in brain [26]. The minor allele of rs2070902 was associated with increased expression of *FCER1G* in blood [26].

Conclusions

This study represents a test of the hypothesis that rs2070902 modulated splicing of *FCER1G* exon 2 in human brain. Our results do not support this hypothesis although we did find that *FCER1G* is robustly expressed in microglia and that the proportion of *FCER1G* expressed as the *D2-FCER1G* isoform is increased in brain samples with high AD neuropathology. Overall, these studies add to our understanding of *FCER1G* expression and splicing in particular and AD genetic mechanisms in general.

ACKNOWLEDGMENTS

The authors acknowledge Susan Kraner, Ph.D., for her helpful consultations regarding immunohistochemistry.

FUNDING

This research was funded by NIH, grant numbers RF1AG059717 (SE) and R21AG068370 (SE).

CONFLICT OF INTEREST

The authors declare no conflict of interest.

DATA AVAILABILITY

The data supporting the findings of this study are available within the article.

REFERENCES

[1] Wightman DP, Jansen IE, Savage JE, Shadrin AA, Bahrami S, Holland D, Rongve A, Borte S, Winsvold BS, Drange OK, Martinsen AE, Skogholt AH, Willer C, Brathen G, Bosnes I, Nielsen JB, Fritsche LG, Thomas LF, Pedersen LM, Gabrielsen ME, Johnsen MB, Meisingset TW, Zhou W, Proitsi P, Hodges A, Dobson R, Velayudhan L, Heilbron K, Auton A, andMe Research T, Sealock JM, Davis LK, Pedersen NL, Reynolds CA, Karlsson IK, Magnusson S, Stefansson H, Thordardottir S, Jonsson PV, Snaedal J, Zettergren A, Skoog I, Kern S, Waern M, Zetterberg H, Blennow K, Stordal E, Hveem K, Zwart JA, Athanasiu L, Selnes P, Saltvedt I, Sando SB, Ulstein I, Djurovic S, Fladby T, Aarsland D, Selbaek G, Ripke S, Stefansson K, Andreassen OA, Posthuma D (2021) A genome-wide association study with 1,126,563 individuals identifies new risk loci for Alzheimer's disease. *Nat Genet* **53**, 1276-1282.

[2] Schwartzentruber J, Cooper S, Liu JZ, Barrio-Hernandez I, Bello E, Kumasaka N, Young AMH, Franklin RJM, Johnson T, Estrada K, Gaffney DJ, Beltrao P, Bassett A (2021) Genome-wide meta-analysis, fine-mapping and integrative prioritization implicate new Alzheimer's disease risk genes. *Nat Genet* **53**, 392-402.

[3] Jansen IE, Savage JE, Watanabe K, Bryois J, Williams DM, Steinberg S, Sealock J, Karlsson IK, Hagg S, Athanasiu L, Voyle N, Proitsi P, Witoelar A, Stringer S, Aarsland D, Almdahl IS, Andersen F, Bergh S, Bettella F, Bjornsson S, Braekhus A, Brathen G, de Leeuw C, Desikan RS, Djurovic S, Dumitrescu L, Fladby T, Hohman TJ, Jonsson PV, Kiddle SJ, Rongve A, Saltvedt I, Sando SB, Selbaek G, Shoai M, Skene NG, Snaedal J, Stordal E, Ulstein ID, Wang Y, White LR, Hardy J, Hjerling-Leffler J, Sullivan PF, van der Flier WM, Dobson R, Davis LK, Stefansson H, Stefansson K, Pedersen NL, Ripke S, Andreassen OA, Posthuma D (2019) Genome-wide meta-analysis identifies new loci and functional pathways influencing Alzheimer's disease risk. *Nat Genet* **51**, 404-413.

[4] Wijsman EM, Pankratz ND, Choi Y, Rothstein JH, Faber KM, Cheng R, Lee JH, Bird TD, Bennett DA, Diaz-Arrastia R, Goate AM, Farlow M, Ghetti B, Sweet RA, Foroud TM, Mayeux R (2011) Genome-wide association of familial late-onset Alzheimer's disease replicates BIN1 and CLU and nominates CUGBP2 in interaction with APOE. *PLoS Genet* **7**, e1001308.

[5] Lambert JC, Heath S, Even G, Campion D, Sleegers K, Hiltunen M, Combarros O, Zelenika D, Bullido MJ, Tavernier B, Letenneur L, Bettens K, Berr C, Pasquier F, Fievet N, Barberger-Gateau P, Engelborghs S, De Deyn P, Mateo I, Franck A, Helisalmi S, Porcellini E, Hanon O, de Pancorbo MM, Lendon C, Dufouil C, Jaillard C, Leveillard T, Alvarez V, Bosco P, Mancuso M, Panza F, Nacmias B, Bossu P, Piccardi P, Annoni G, Seripa D, Galimberti D, Hannequin D, Licastro F, Soininen H, Ritchie K, Blanche H, Dartigues JF, Tzourio C, Gut I, Van Broeckhoven C, Alperovitch A, Lathrop M, Amouyel P (2009) Genome-wide association study identifies variants at CLU and CR1 associated with Alzheimer's disease. *Nat Genet* **41**, 1094-1099.

[6] Harold D, Abraham R, Hollingworth P, Sims R, Gerrish A, Hamshere ML, Pahwa JS, Moskvina V, Dowzell K, Williams A, Jones N, Thomas C, Stretton A, Morgan AR, Lovestone S, Powell J, Proitsi P, Lupton MK, Brayne C, Rubinsztein DC, Gill M, Lawlor B, Lynch A, Morgan K, Brown KS, Passmore PA, Craig D, McGuinness B, Todd S, Holmes C, Mann D, Smith AD, Love S, Kehoe PG, Hardy J, Mead S, Fox N, Rossor M, Collinge J, Maier W, Jessen F, Schurmann B, van den Bussche H, Heuser I, Kornhuber J, Wiltfang J, Dichgans M, Frolich L, Hampel H, Hull M, Rujescu D, Goate AM, Kauwe JS, Cruchaga C, Nowotny P, Morris JC, Mayo K, Sleegers K, Bettens K, Engelborghs S, De Deyn PP, Van Broeckhoven C, Livingston G, Bass NJ, Gurling H, McQuillin A, Gwilliam R, Deloukas P, Al-Chalabi A, Shaw CE, Tsolaki M, Singleton AB, Guerreiro R, Muhleisen TW, Nothen MM, Moebus S, Jockel KH, Klopp N, Wichmann HE, Carrasquillo MM, Pankratz VS, Younkin SG, Holmans PA, O'Donovan M, Owen MJ, Williams J (2009) Genome-wide association study identifies variants at CLU and PICALM associated with Alzheimer's disease. *Nat Genet* **41**, 1088-1093.

[7] Brandsma AM, Hogarth PM, Nimmerjahn F, Leusen JH (2016) Clarifying the confusion between cytokine and Fc receptor common gamma chain. *Immunity* **45**, 225-226.

[8] Miyake Y, Toyonaga K, Mori D, Kakuta S, Hoshino Y, Oyamada A, Yamada H, Ono K, Suyama M, Iwakura Y, Yoshikai Y, Yamasaki S (2013) C-type lectin MCL is an FcRgamma-coupled receptor that mediates the adjuvanticity of mycobacterial cord factor. *Immunity* **38**, 1050-1062.

[9] Zhang Y, Chen K, Sloan SA, Bennett ML, Scholze AR, O'Keeffe S, Phatnani HP, Guarnieri P, Caneda C, Ruderisch N, Deng S, Liddelow SA, Zhang C, Daneman R, Maniatis T, Barres BA, Wu JQ (2014) An RNA-sequencing transcriptome and splicing database of glia, neurons, and vascular cells of the cerebral cortex. *J Neurosci* **34**, 11929-11947.

[10] Jay TR, von Saucken VE, Landreth GE (2017) TREM2 in neurodegenerative diseases. *Mol Neurodegener* **12**, 56.

[11] Matarin M, Salih DA, Yasvoina M, Cummings DM, Guelfi S, Liu W, Nahaboo Solim MA, Moens TG, Paublete RM, Ali SS, Perona M, Desai R, Smith KJ, Latcham J, Fulleylove M, Richardson JC, Hardy J, Edwards FA (2015) A genome-wide gene-expression analysis and database in transgenic mice during development of amyloid or tau pathology. *Cell Rep* **10**, 633-644.

[12] Lambracht-Washington D, Fu M, Hynan LS, Rosenberg RN (2021) Changes in the brain transcriptome after DNA Abeta42 trimer immunization in a 3xTg-AD mouse model. *Neurobiol Dis* **148**, 105221.

[13] Keren-Shaul H, Spinrad A, Weiner A, Matcovitch-Natan O, Dvir-Szternfeld R, Ulland TK, David E, Baruch K, Lara-Astaiso D, Toth B, Itzkovitz S, Colonna M, Schwartz M, Amit I (2017) A unique microglia type associated with restricting development of Alzheimer's disease. *Cell* **169**, 1276-1290 e1217.

[14] Grear KE, Ling IF, Simpson JF, Furman JL, Simmons CR, Peterson SL, Schmitt FA, Markesbery WR, Liu Q, Crook JE, Younkin SG, Bu G, Estus S (2009) Expression of SORL1 and a novel SORL1 splice variant in normal and Alzheimers disease brain. *Mol Neurodegener* **4**, 46.

[15] Malik M, Chiles J, 3rd, Xi HS, Medway C, Simpson J, Potluri S, Howard D, Liang Y, Paumi CM, Mukherjee S, Crane P, Younkin S, Fardo DW, Estus S (2015) Genetics of CD33 in Alzheimer's disease and acute myeloid leukemia. *Hum Mol Genet* **24**, 3557-3570.

[16] Shaw BC, Katsumata Y, Simpson JF, Fardo DW, Estus S (2021) Analysis of genetic variants associated with levels of immune modulating proteins for impact on Alzheimer's disease risk reveal a potential role for SIGLEC14. *Genes (Basel)* **12**, 1008.

[17] Shaw BC, Snider HC, Turner AK, Zajac DJ, Simpson JF, Estus S (2022) An alternatively spliced TREM2 isoform

lacking the ligand binding domain is expressed in human brain. *J Alzheimers Dis* **87**, 1647-1657.

[18] Tan RH, Pok K, Wong S, Brooks D, Halliday GM, Kril JJ (2013) The pathogenesis of cingulate atrophy in behavioral variant frontotemporal dementia and Alzheimer's disease. *Acta Neuropathol Commun* **1**, 30.

[19] Nelson PT, Braak H, Markesbery WR (2009) Neuropathology and cognitive impairment in Alzheimer disease: A complex but coherent relationship. *J Neuropathol Exp Neurol* **68**, 1-14.

[20] Malik M, Simpson JF, Parikh I, Wilfred BR, Fardo DW, Nelson PT, Estus S (2013) CD33 Alzheimer's risk-altering polymorphism, CD33 expression, and exon 2 splicing. *J Neurosci* **33**, 13320-13325.

[21] Akiyama H, McGeer PL (1990) Brain microglia constitutively express beta-2 integrins. *J Neuroimmunol* **30**, 81-93.

[22] Peress NS, Fleit HB, Perillo E, Kuljis R, Pezzullo C (1993) Identification of Fc gamma RI, II and III on normal human brain ramified microglia and on microglia in senile plaques in Alzheimer's disease. *J Neuroimmunol* **48**, 71-79.

[23] Olah M, Patrick E, Villani AC, Xu J, White CC, Ryan KJ, Piehowski P, Kapasi A, Nejad P, Cimpean M, Connor S, Yung CJ, Frangieh M, McHenry A, Elyaman W, Petyuk V, Schneider JA, Bennett DA, De Jager PL, Bradshaw EM (2018) A transcriptomic atlas of aged human microglia. *Nat Commun* **9**, 539.

[24] Cunningham F, Allen JE, Allen J, Alvarez-Jarreta J, Amode MR, Armean IM, Austine-Orimoloye O, Azov AG, Barnes I, Bennett R, Berry A, Bhai J, Bignell A, Billis K, Boddu S, Brooks L, Charkhchi M, Cummins C, Da Rin Fioretto L, Davidson C, Dodiya K, Donaldson S, El Houdaigui B, El Naboulsi T, Fatima R, Giron CG, Genez T, Martinez JG, Guijarro-Clarke C, Gymer A, Hardy M, Hollis Z, Hourlier T, Hunt T, Juettemann T, Kaikala V, Kay M, Lavidas I, Le T, Lemos D, Marugan JC, Mohanan S, Mushtaq A, Naven M, Ogeh DN, Parker A, Parton A, Perry M, Pilizota I, Prosovetskaia I, Sakthivel MP, Salam AIA, Schmitt BM, Schuilenburg H, Sheppard D, Perez-Silva JG, Stark W, Steed E, Sutinen K, Sukumaran R, Sumathipala D, Suner MM, Szpak M, Thormann A, Tricomi FF, Urbina-Gomez D, Veidenberg A, Walsh TA, Walts B, Willhoft N, Winterbottom A, Wass E, Chakiachvili M, Flint B, Frankish A, Giorgetti S, Haggerty L, Hunt SE, GR II, Loveland JE, Martin FJ, Moore B, Mudge JM, Muffato M, Perry E, Ruffier M, Tate J, Thybert D, Trevanion SJ, Dyer S, Harrison PW, Howe KL, Yates AD, Zerbino DR, Flicek P (2022) Ensembl 2022. *Nucleic Acids Res* **50**, D988-D995.

[25] McAleese SM, Miller HR (2003) Cloning and sequencing of the equine and ovine high-affinity IgE receptor beta-and gamma-chain cDNA. *Immunogenetics* **55**, 122-125.

[26] Consortium GT (2013) The Genotype-Tissue Expression (GTEx) project. *Nat Genet* **45**, 580-585.

[27] Walter S, Jumpertz T, Huttenrauch M, Ogorek I, Gerber H, Storck SE, Zampar S, Dimitrov M, Lehmann S, Lepka K, Berndt C, Wiltfang J, Becker-Pauly C, Beher D, Pietrzik CU, Fraering PC, Wirths O, Weggen S (2019) The metalloprotease ADAMTS4 generates N-truncated Abeta4-x species and marks oligodendrocytes as a source of amyloidogenic peptides in Alzheimer's disease. *Acta Neuropathol* **137**, 239-257.

[28] Silva AL, Romao L (2009) The mammalian nonsense-mediated mRNA decay pathway: To decay or not to decay! Which players make the decision? *FEBS Lett* **583**, 499-505.

[29] Peixeiro I, Inacio A, Barbosa C, Silva AL, Liebhaber SA, Romao L (2012) Interaction of PABPC1 with the translation initiation complex is critical to the NMD resistance of AUG-proximal nonsense mutations. *Nucleic Acids Res* **40**, 1160-1173.

[30] Neu-Yilik G, Amthor B, Gehring NH, Bahri S, Paidassi H, Hentze MW, Kulozik AE (2011) Mechanism of escape from nonsense-mediated mRNA decay of human beta-globin transcripts with nonsense mutations in the first exon. *RNA* **17**, 843-854.

[31] Inacio A, Silva AL, Pinto J, Ji X, Morgado A, Almeida F, Faustino P, Lavinha J, Liebhaber SA, Romao L (2004) Nonsense mutations in close proximity to the initiation codon fail to trigger full nonsense-mediated mRNA decay. *J Biol Chem* **279**, 32170-32180.

[32] Takai T, Li M, Sylvestre D, Clynes R, Ravetch JV (1994) FcR gamma chain deletion results in pleiotrophic effector cell defects. *Cell* **76**, 519-529.

[33] Geijtenbeek TB, Gringhuis SI (2009) Signalling through C-type lectin receptors: Shaping immune responses. *Nat Rev Immunol* **9**, 465-479.

[34] Nimmerjahn F, Ravetch JV (2008) Anti-inflammatory actions of intravenous immunoglobulin. *Annu Rev Immunol* **26**, 513-533.